A Two-Temperature Model Based on Fin-Approximation for Transient Longitudinal Heat Transfer in Unidirectional Composite

Gilles Dusserre

Key Engineering Materials
ISSN: 1662-9795, Vol. 926, pp 1882-1889
doi:10.4028/p-2m7u9s

Submitted: 2021-12-08
Revised: 2022-01-28
Accepted: 2022-02-02
Online: 2022-07-22

A Two-Temperature Model Based on Fin-Approximation for Transient Longitudinal Heat Transfer in Unidirectional Composite

Gilles Dusserre[1,a*]

[1]Institut Clément Ader (ICA) ; Université de Toulouse ; CNRS, IMT Mines Albi, INSA, ISAE-SUPAERO, UPS ; Campus Jarlard, F-81013 Albi, France

[a]gilles.dusserre@mines-albi.fr

Keywords: Heat transfer; fin-approximation; high interfacial thermal resistance

Abstract. The reliability of a two-temperature model is assessed in the case of longitudinal heat transfer in unidirectional composites. One interest is that it makes it possible to apply separate boundary conditions or source terms on the fibre and the matrix (emissivity for example), without necessitating an explicit description of the fibre and matrix domains. For the sake of simplicity, the model under study is based on a fin-approximation in both fibre and matrix, which implies a high interfacial thermal resistance. The range of validity of this assumption is investigated by comparing the model to an axisymmetric one-temperature model, using non-dimension variables and Dirichlet boundary conditions. It turns out that this range of validity is strongly dependent on the parameters.

Introduction

Heat transfer in composites is usually computed based on homogenization approaches, either at micro- [1-3], meso- or macro-scale [4]. High interfacial resistance between highly conductive fibre and low conductive matrix may result in a difference of temperature between the fibre and the surrounding matrix during fast transient heat transfer, which are neglected by the usual homogenisation methods. This can be accounted for at the macro-scale by two-temperature models, which consider the composite as a single-phase continuum whose state is described by a separate temperature field for each phase [5]. For instance, such approaches successfully describe heat transfer in phase-change materials [6]. Thanks to the high thermal conductivity and the low radius of the fibre, a fin-approximation is likely to be reliable in the fibre provided that the interfacial thermal resistance is high enough. For very high interfacial thermal resistance and high fibre volume fraction (V_f), the fin-approximation is likely to be reliable even in the surrounding matrix. This assumption is not of general purpose, but can be of interest for some composites, for instance carbon-geopolymer composites with interfacial porosity, as illustrated in [7], which implies initial high interfacial resistance likely to increase with fibre/matrix decohesion in damaged composites. Moreover, such composites can be hardened by Joule heating thanks to the high electrical conductivity of the carbon fibres [8]. Solving this specific problem involving different heat sources in the fibre (Joule effect) and in the matrix (Joule effect and exothermic hardening [9]), together with temperature dependent kinetics and material properties (geopolymer electrical resistivity for instance [10]) would benefit from considering the temperature difference between fibre and matrix. Moreover, if the above-mentioned assumptions are met, the additional computational cost would be low. This paper investigates the suitability of this model for longitudinal heat conduction in a unidirectional composite (Fig. 1) in order to provide insight about its applicability to specific problems.

Investigation of the Range of Validity

Problem schematization. The problem addressed in this paper involves a cylindrical fibre of radius $\boldsymbol{R_f}$, surrounded by a layer of matrix of uniform thickness (Fig. 2), resulting in a fibre volume fraction $\boldsymbol{V_f}$. The problem is defined in a cylindrical coordinate system. A contact heat conductance $\boldsymbol{h}$ is defined at the fibre/matrix interface ($\boldsymbol{r = R_f}$) and the outer boundary of the matrix ($\boldsymbol{r = R = \frac{R_f}{\sqrt{V_f}}}$) is adiabatic to roughly simulate longitudinal heat transfer at the macro-scale. Boundary conditions are

assigned at both extremities of the domain (z=0 and z=Z). The initial temperature is $\boldsymbol{T_0}$ in the whole domain. The matrix is isotropic, whereas the fibre is considered as an orthotropic material, with different conductivity in the axial and radial directions.

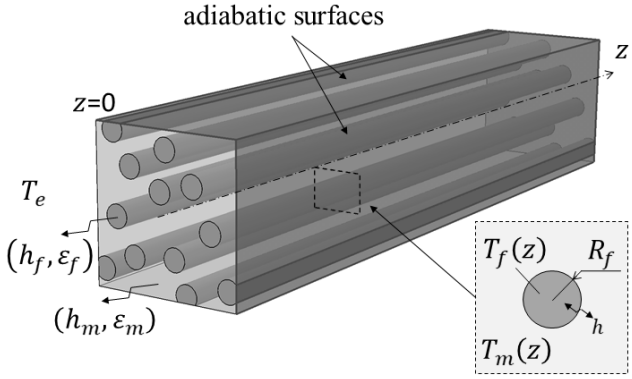

Fig. 1. Schematic view of the one-dimensional problem

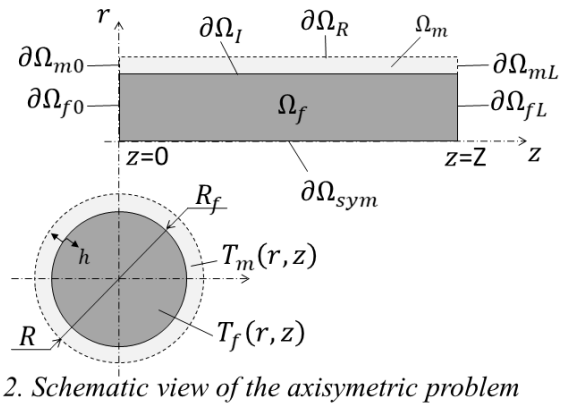

Fig. 2. Schematic view of the axisymetric problem

One-temperature two-dimension axisymmetric model (1T2D). The reference solution for this problem is obtained with a usual one-temperature model, involving a single temperature field $T(r,z,t)$ defined in the whole domain $\Omega_f \cup \Omega_m$. The first case study involves Dirichlet boundary conditions.

Heat equation. The heat balance is obtained by Eq. (1) in the fibre and the matrix, where s is a volumetric heat source.

$$\begin{cases} \rho C_P \frac{\partial T}{\partial t} = \frac{1}{r}\frac{\partial}{\partial r}\left(k_r r \frac{\partial T}{\partial r}\right) + \frac{\partial}{\partial z}\left(k_z \frac{\partial T}{\partial z}\right) + s \quad \forall\, M(r,z) \in \Omega_f, \forall t \\ \rho_m C_{Pm} \frac{\partial T}{\partial t} = \frac{1}{r}\frac{\partial}{\partial r}\left(k_m r \frac{\partial T}{\partial r}\right) + \frac{\partial}{\partial z}\left(k_m \frac{\partial T}{\partial z}\right) + s \quad \forall\, M(r,z) \in \Omega_m, \forall t \end{cases} \tag{1}$$

Initial conditions. The initial temperature is constant in the whole domain Eq. (2).

$$T(r,z,0) = T_0 \quad \forall\, M(r,z) \in \Omega_f \cup \Omega_m \tag{2}$$

Dirichlet boundary conditions. The temperature is fixed at the extremities of the domain Eq. (3). At $t = 0$, the temperature at $z = 0$ is instantaneously set to T_e.

$$\begin{cases} T = T_e \quad \forall\, M(r,0) \in \partial\Omega_{f0} \cup \partial\Omega_{m0}, \forall t \in \mathbb{R}_+^* \\ T = T_0 \quad \forall\, M(r,Z) \in \partial\Omega_{fL} \cup \partial\Omega_{mL}, \forall t \in \mathbb{R}_+ \end{cases} \tag{3}$$

Fibre-matrix interface. The heat flux density at the fibre-matrix interface is given in Eq. (4), where R_f^- and R_f^+ are the radial coordinate of the interface ($r = R_f$) respectively in the fibre and the matrix.

$$\vec{q} = h\left[T\left(R_f^-, z, t\right) - T\left(R_f^+, z, t\right)\right]\vec{e}_r = -k_r \frac{\partial T}{\partial r}\Big|_{r=R_f^-,z,t} \vec{e}_r = -k_m \frac{\partial T}{\partial r}\Big|_{r=R_f^+,z,t} \vec{e}_r \tag{4}$$

Non-dimension model. Let $\bar{T}$ be the non-dimension temperature defined as $T = T_e + (T_0 - T_e)\bar{T}$. Let $\bar{t}$, $\bar{r}$ and $\bar{z}$ be respectively the non-dimension time and coordinates, defined as $t = \tau\bar{t}$, $r = \frac{R_f}{2}\bar{r}$ and $z = L\bar{z}$ (thus $Z = L\bar{Z}$), with $\tau = \frac{\rho C_P L^2}{k_z}$. Let $\bar{s} = \frac{L^2}{k_z}\frac{s}{T_0 - T_e}$ be the non-dimension source term. Eq. (1-3) reduce to Eq. (5-7) respectively, assuming temperature-independent conductivity. L will be defined later. This non-dimension problem is schematized in Fig. 3.

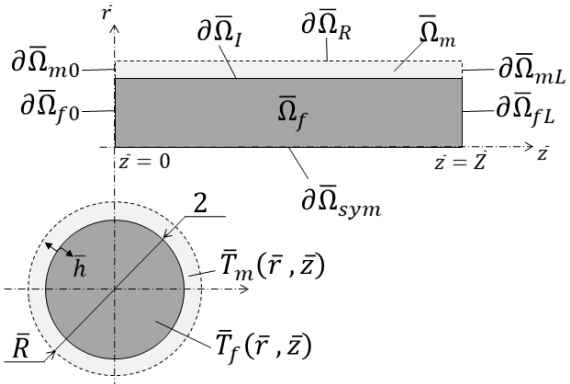

Fig. 3. Schematic view of non-dimension 1T2D model

$$\begin{cases} \dfrac{\partial\bar{T}}{\partial\bar{t}} = \bar{k}_r \dfrac{1}{\bar{r}}\dfrac{\partial}{\partial\bar{r}}\left(\bar{r}\dfrac{\partial\bar{T}}{\partial\bar{r}}\right) + \dfrac{\partial^2\bar{T}}{\partial\bar{z}^2} + \bar{s} \quad \forall\, \bar{M}(\bar{r},\bar{z}) \in \bar{\Omega}_f, \forall\bar{t} \\ \overline{\rho_m C_{Pm}}\dfrac{\partial\bar{T}}{\partial\bar{t}} = \bar{k}_{rm}\dfrac{1}{\bar{r}}\dfrac{\partial}{\partial\bar{r}}\left(\bar{r}\dfrac{\partial\bar{T}}{\partial\bar{r}}\right) + \bar{k}_{zm}\dfrac{\partial^2\bar{T}}{\partial\bar{z}^2} + \bar{s} \quad \forall\, \bar{M}(\bar{r},\bar{z}) \in \bar{\Omega}_m, \forall\bar{t} \end{cases} \tag{5}$$

$$\bar{T}(\bar{r},\bar{z},0) = 0 \quad \forall\, \bar{M}(\bar{r},\bar{z}) \in \bar{\Omega}_f \cup \bar{\Omega}_m \tag{6}$$

$$\begin{cases} \bar{T} = 1 \quad \forall\, \bar{M}(\bar{r},0) \in \partial\bar{\Omega}_{f0} \cup \partial\bar{\Omega}_{m0}, \forall\bar{t} \in \mathbb{R}_+^* \\ \bar{T} = 0 \quad \forall\, \bar{M}(\bar{r},\bar{Z}) \in \partial\bar{\Omega}_{fL} \cup \partial\bar{\Omega}_{mL}, \forall\bar{t} \in \mathbb{R}_+ \end{cases} \tag{7}$$

The non-dimension radial conductivity of the fibre and the matrix are respectively $\bar{k}_r = \frac{4L^2}{R_f^2}\frac{k_r}{k_z}$ and $\bar{k}_{rm} = \frac{k_m}{k_z}\frac{4L^2}{R_f^2}$, the non-dimension axial conductivity and specific heat of the matrix are respectively $\bar{k}_{zm} = \frac{k_m}{k_z}$ and $\overline{\rho_m C_{Pm}} = \frac{\rho_m C_{Pm}}{\rho C_P}$.

It is noteworthy that in the non-dimension coordinate system, both fibre and matrix may have orthotropic conductivity.

In the non-dimension model, Eq. (4) writes as Eq. (8), which defines the non-dimension contact heat conductance at the interface, $\bar{h}$ (Eq. (9)).

$$\bar{h}[\bar{T}(1^-,\bar{z},\bar{t}) - \bar{T}(1^+,\bar{z},\bar{t})] = -\bar{k}_r\frac{\partial\bar{T}}{\partial\bar{r}}_{|1^-,\bar{z},\bar{t}} = -\bar{k}_{rm}\frac{\partial\bar{T}}{\partial\bar{r}}_{|1^+,\bar{z},\bar{t}} \tag{8}$$

$$\bar{h} = \frac{2L^2}{R_f}\frac{1}{k_z}h \tag{9}$$

Two-temperature one-dimension model (2T1D). The same problem is solved by a two-temperature 1D model, assuming that both fibre and matrix are thermally thin. This assumption is meaningful provided that the Biot number in the fibre, Bi_f (Eq. (10)) and in the matrix, Bi_m (Eq. (11)) are together low. This assumption implies that the 2D heat transfer described previously reduces to a 1D heat transfer, in which the radial heat flux at the fibre-matrix interface is instantaneously diffused into each subdomain Ω_f and Ω_m. It is therefore accounted for by a source term in the heat equation.

$$Bi_f = \frac{R_f}{2}\frac{h}{k_r} \tag{10}$$

$$Bi_m = \frac{R_f}{2}\frac{h}{k_m}\frac{1-V_f}{V_f} \tag{11}$$

It is noteworthy that the definition of Bi_m corresponds to the axisymmetric conditions described in Fig. 2, but is only a rough approximation in an actual configuration as described in Fig. 1.

Heat equation. Under such assumptions, Eq. (1) writes as Eq. (12), where the cross-section averaged temperature field is denoted T_f in the fibre and T_m in the matrix.

$$\begin{cases} \rho C_P \frac{\partial T_f}{\partial t} = k_z \frac{\partial^2 T_f}{\partial z^2} - h \frac{2}{R_f}\left(T_f - T_m\right) + s_f \quad \forall z \in [0, Z], \forall t \\ \rho_m C_{Pm} \frac{\partial T_m}{\partial t} = k_m \frac{\partial^2 T_m}{\partial z^2} + h \frac{2}{R_f}\left(T_f - T_m\right) \frac{V_f}{1-V_f} + s_m \quad \forall z \in [0, Z], \forall t \end{cases} \tag{12}$$

Non-dimension model. Using the non-dimension parameters used in the previous model ($\hat{T}(\bar{z}, \bar{t})$ and $\tilde{T}(\bar{z}, \bar{t})$ are respectively the non-dimension temperatures related to T_f and T_m) and taking L as $L^2 = \frac{k_z R_f}{2h}$, Eq. (12) reduces to Eq. (13), with $\hat{s} = \frac{s_f}{T_0 - T_e} \frac{L^2}{k_z}$ and $\tilde{s} = \frac{s_m}{T_0 - T_e} \frac{L^2}{k_z}$. The initial and boundary conditions are given by Eq. (14) and Eq. (15) respectively. In such conditions, the non-dimension radial conductivity of the fibre and the matrix are respectively $\bar{k}_r = \frac{1}{Bi_f}$ and $\bar{k}_{rm} = \frac{1-V_f}{V_f} \frac{1}{Bi_m}$. The non-dimension contact heat conductance at the interface reduces to $\bar{h} = 1$.

$$\begin{cases} \frac{\partial \hat{T}}{\partial \bar{t}} = \frac{\partial^2 \hat{T}}{\partial \bar{z}^2} - \left(\hat{T} - \tilde{T}\right) + \hat{s} \quad \forall \bar{z} \in [0; \bar{z}], \forall \bar{t} \\ \overline{\rho_m C_{Pm}} \frac{\partial \tilde{T}}{\partial \bar{t}} = \bar{k}_{zm} \frac{\partial^2 \tilde{T}}{\partial \bar{z}^2} + \left(\hat{T} - \tilde{T}\right) \frac{V_f}{1-V_f} + \tilde{s} \quad \forall \bar{z} \in [0; \bar{z}], \forall \bar{t} \end{cases} \tag{13}$$

$$\hat{T}(\bar{z}, 0) = \tilde{T}(\bar{z}, 0) = 0 \quad \forall\, \bar{z} \in [0; \bar{Z}] \tag{14}$$

$$\begin{cases} \hat{T}(0, \bar{t}) = \tilde{T}(0, \bar{t}) = 1 \quad \forall \bar{t} \in \mathbb{R}_+^* \\ \hat{T}(\bar{Z}, \bar{t}) = \tilde{T}(\bar{Z}, \bar{t}) = 0 \quad \forall \bar{t} \in \mathbb{R}_+ \end{cases} \tag{15}$$

Numerical application. The reference solution computed from 2T1D model is compared with the results of 1T2D model in order to assess the conditions in which the latter model is suitable. The following assumptions are considered in this section:

- No volume heat sources are considered.
- The ratio $\frac{\rho_m C_{Pm}}{\rho C_P}$ is not expected to vary significantly for most material couple and is set to 1.
- The fibre volume fraction is set to $V_f = 60\%$, a usual order of magnitude inside a tow. The non-dimension outer matrix radius is $\bar{R} = \frac{2}{\sqrt{V_f}}$.

In such conditions, the 1T2D model (Eq. (5-7,9)) reduces to Eq. (16,6,7,17) and the 2T1D model (Eq. (13-15)) reduces to Eq. (18,13,14). The 1T2D solution depends on three parameters, Bi_f, $\frac{k_r}{k_z}$ and $\frac{k_m}{k_z}$, whereas only the latter is involved in the 2T1D model.

$$\begin{cases} \frac{\partial \bar{T}}{\partial \bar{t}} = \bar{k}_r \frac{1}{\bar{r}} \frac{\partial}{\partial \bar{r}}\left(\bar{r} \frac{\partial \bar{T}}{\partial \bar{r}}\right) + \frac{\partial^2 \bar{T}}{\partial \bar{z}^2} \quad \forall\, \bar{M}(\bar{r}, \bar{z}) \in \bar{\Omega}_f, \forall \bar{t} \\ \frac{\partial \bar{T}}{\partial \bar{t}} = \bar{k}_{rm} \frac{1}{\bar{r}} \frac{\partial}{\partial \bar{r}}\left(\bar{r} \frac{\partial \bar{T}}{\partial \bar{r}}\right) + \bar{k}_{zm} \frac{\partial^2 \bar{T}}{\partial \bar{z}^2} \quad \forall\, \bar{M}(\bar{r}, \bar{z}) \in \bar{\Omega}_m, \forall \bar{t} \end{cases} \tag{16}$$

$$\bar{T}(1^-, \bar{z}, \bar{t}) - \bar{T}(1^+, \bar{z}, \bar{t}) = -\bar{k}_r \frac{\partial \bar{T}}{\partial \bar{r}_{|1^-, \bar{z}, \bar{t}}} = -\bar{k}_{rm} \frac{\partial \bar{T}}{\partial \bar{r}_{|1^+, \bar{z}, \bar{t}}} \tag{17}$$

$$\begin{cases} \frac{\partial \hat{T}}{\partial \bar{t}} = \frac{\partial^2 \hat{T}}{\partial \bar{z}^2} - \left(\hat{T} - \tilde{T}\right) \quad \forall \bar{z} \in [0, \bar{Z}], \forall \bar{t} \\ \frac{\partial \tilde{T}}{\partial \bar{t}} = \bar{k}_{zm} \frac{\partial^2 \tilde{T}}{\partial \bar{z}^2} + \left(\hat{T} - \tilde{T}\right) \frac{V_f}{1-V_f} \quad \forall \bar{z} \in [0, \bar{Z}], \forall \bar{t} \end{cases} \tag{18}$$

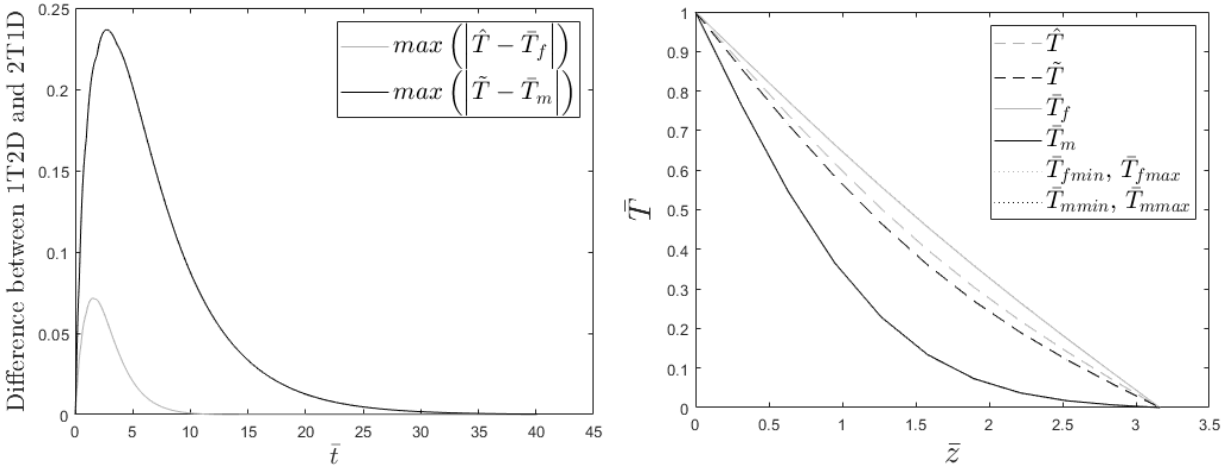

a. *b.*

Fig. 4. 1T2D and 2D1T results for $\bar{Z} = 3.16$, $Bi_f = 5 \cdot 10^{-4}$, $\frac{k_r}{k_z} = 1$ and $\frac{k_m}{k_z} = 0.2$; (a.) maximum gap between average temperature; (b.) temperature fields along $\bar{z}$-axis when the gap is maximum

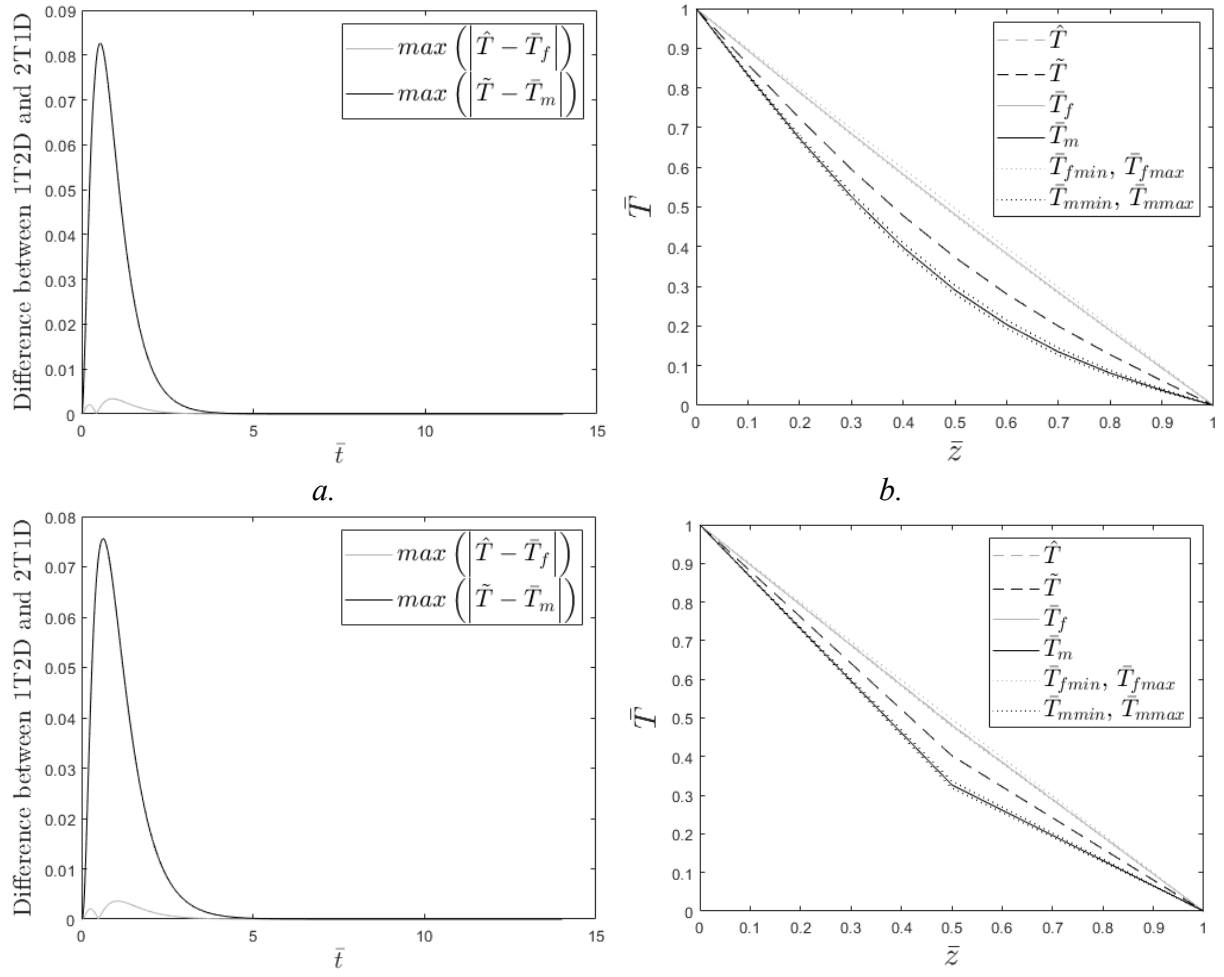

a. *b.*

c. *d.*

Fig. 5. 1T2D and 2D1T results for $\bar{Z} = 1$, $Bi_f = 5 \cdot 10^{-2}$, $\frac{k_r}{k_z} = 1$ and $\frac{k_m}{k_z} = 0.2$; (a. and c.) maximum gap between average temperature; (b. and d.) temperature fields along $\bar{z}$-axis when the gap is maximum with (a. and b.) 11 and (c. and d.) 3 nodes

1T2D and 2T1D models were computed thanks to a 1D or 2D finite difference scheme for several Bi_f and $\bar{Z}$ values, with $\frac{k_r}{k_z} = 1$ (isotropic fibre) and $\frac{k_m}{k_z} = 0.02$ or $\frac{k_m}{k_z} = 0.2$ (representative of carbon/geopolymer composites assuming $k_z = 5$ W.m^{-1}.K^{-1} and $0.1 < k_m < 1$ W.m^{-1}.K^{-1}). The simulation duration, $\bar{t}_{max}$, was chosen in such a way to catch the maximum gap between fibre and matrix average temperature obtained with both models, Eq. (19).

$$\bar{t}_{max} \approx \min\left(\bar{Z}^2 \frac{k_z}{k_m}; \bar{Z}^2 + 4Bi_f \left(\frac{2}{\sqrt{V_f}} - 1\right)^2 \frac{k_r}{k_m}\right) \tag{19}$$

Some examples of the results obtained with the following parameters are plotted in Fig. 4 and 5. In most cases, the discrepancy tends toward zero at the end of the computations. It turns out that the initial postulate stating that the 2T1D model would provide accurate results with low Biot numbers is not straightforward. Indeed, the assumption of thermally thin fibre and matrix is very well verified in Fig. 4.b, where the minimum and maximum temperatures computed are superposed with the average temperatures. Nonetheless, large differences are found between both models.

Actually, the most sensitive parameter is the length $\bar{Z}$, as illustrated in Fig. 6, where the maximum gap in both fibre and matrix is reported as a function of Bi_f and $\bar{Z}$ for $\frac{k_m}{k_z} = 0.2$ and $\frac{k_m}{k_z} = 0.02$.

Discussion

Fig. 6 provides the validity map of the model, mainly characterised by low $\bar{Z}$ values and depending on the other parameters. The length-scale, L, and time-scale, τ, of the problem are very low for usual applications, typically lower than 1 mm and 1s respectively, and it may be concluded that the model would not be useful for usual application at the macro-scale. At a time-scale larger than a few τ, Fig. 4 and Fig. 5 show that both models provide the same results, actually because fibre and matrix temperatures are very close, which finally opens a new validity range of the 2T1D model. In this case, the proposed model could provide a new insight onto microscopic scale, for example the heat transfer between fibre and matrix, which is necessarily null in a homogenized approach. The following case study investigates the model capability to apply separate heat source on fibres and matrix.

Case study: hardening by Joule heating

Heating by Joule effect in conductive carbon fibers is a way toward geopolymer matrix hardening [8]. The electric potential gradient, $\frac{\partial U}{\partial z}$, is assumed to be constant over the UD sample, i.e. the Joule volumetric heating rate is uniform and there is no heat transfer in the sample, except local heat exchange between fiber and matrix, assuming that the above-mentioned assumptions are met. In such conditions, Eq. (12) reduces to Eq. (20), with $s_f = \left(\frac{\partial U}{\partial z}\right)^2 \frac{1}{\rho_e}$ and $s_m = \left(\frac{\partial U}{\partial z}\right)^2 \frac{1}{\rho_{em}}$, where ρ_e and ρ_{em} are respectively the electrical resistivity of fibre and matrix. Adiabatic boundary conditions are assumed. The problem can be written in terms of temperature difference between fibre and matrix, $\Delta T = T_f - T_m$, leading to Eq. (21). Introducing the non-dimension variables $\bar{t}$ and $\overline{\Delta T}$, with $t = \tau \bar{t}$ and $\Delta T = \theta \overline{\Delta T}$, with $\tau = \frac{R_f}{2h\left(\frac{1}{\rho C_P} + \frac{1}{\rho_m C_{Pm}} \frac{V_f}{1-V_f}\right)}$ and $\theta = \tau \left(\frac{\partial U}{\partial z}\right)^2 \left(\frac{1}{\rho C_P \rho_e} - \frac{1}{\rho_m C_{Pm} \rho_{em}}\right)$, leads to Eq. (22).

$$\begin{cases} \rho C_P \frac{\partial T_f}{\partial t} = -h \frac{2}{R_f}\left(T_f - T_m\right) + s_f \quad \forall t \\ \rho_m C_{Pm} \frac{\partial T_m}{\partial t} = h \frac{2}{R_f}\left(T_f - T_m\right) \frac{V_f}{1-V_f} + s_m \quad \forall t \end{cases} \tag{20}$$

$$\frac{\partial \Delta T}{\partial t} = -h \frac{2}{R_f} \Delta T \left(\frac{1}{\rho C_P} + \frac{1}{\rho_m C_{Pm}} \frac{V_f}{1-V_f}\right) + \frac{s_f}{\rho C_P} - \frac{s_m}{\rho_m C_{Pm}} \tag{21}$$

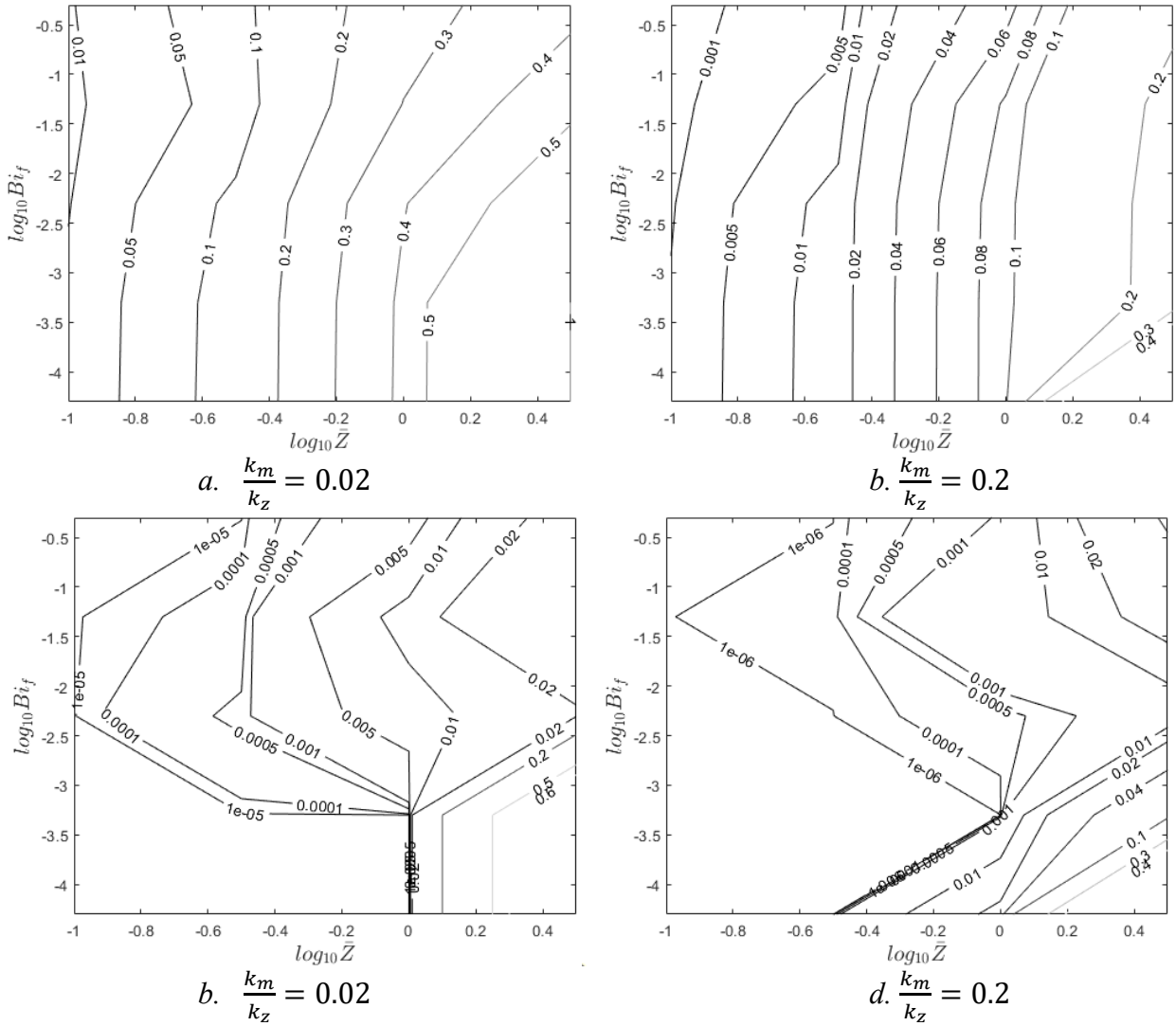

Fig. 6. Maximum gap between (a. and b.) matrix and (c. and d.) fibre temperature computed with 1T2D and 2D1T as a function of $\bar{Z}$ and Bi_f, for $\frac{k_r}{k_z} = 1$.

$$\frac{\partial \overline{\Delta T}}{\partial \bar{t}} = 1 - \overline{\Delta T} \tag{22}$$

With the initial condition $\overline{\Delta T} = 0$ at $\bar{t} = 0$, Eq. (22) reduces to $\overline{\Delta T} = 1 - e^{-\bar{t}}$, i.e. $\overline{\Delta T}$ monotonously increases and tends toward its maximal value $\overline{\Delta T} = 1$. Therefore ΔT tends toward θ. In [8], $\frac{\partial U}{\partial z}$ of value 7.5, 15 and 30 V.m^{-1} ρ_e of value 17 µΩ.m and R_f of value 3.45 µm were considered. ρ_{em} is expected to change significantly during the hardening process, but a minimum value of the order of 1 Ω.m seems to be meaningful [10,11]. Assuming $\frac{\rho C_P}{\rho_m C_{Pm}} \approx 1$, $\frac{\rho_e}{\rho_{em}} \ll 1$ and $\frac{V_f}{1-V_f} \approx 1$, the order of magnitude of ΔT is $\theta = \frac{R_f}{4h}\left(\frac{\partial U}{\partial z}\right)^2 \frac{1}{\rho_e}$.

With $\frac{\partial U}{\partial z} \approx 30$ V.m^{-1}, the maximum value of ΔT is of the order of 1 K if $h \approx 45$ W.m^{-2}.K^{-1}. Even if it is consistent with a low Biot number, this order of magnitude is very low and do not seem to be reliable to cases where both fibre and matrix are actually in contact [12], even with a high interfacial porosity. This order of magnitude would be representative of radiative heat transfer at 400 °C, or convective heat transfer at low pressure in damaged materials without any contact.

Conclusion

The domain of validity of a two-temperature model has been investigated in the case of longitudinal heat transfer in a unidirectional composite with Dirichlet boundary conditions. This domain is two-fold. First at very small time- and length-scale, which are not the scope of usual composite applications. The second domain of validity actually correspond to cases where the temperature difference between fibre and matrix is very low. The low additional computational cost of the model could make it suitable to get a better accuracy in cases involving several temperature-dependent physics in a coupled manner, where neglecting a low temperature difference between fibre and matrix would lead to small errors likely to be amplified during the successive iterations. The case study described above will be extended to a more complex problem with boundary conditions involving heat transfer at the macro-scale, and considering electrical transfer in a matrix of changing resistivity, together with an exothermic hardening kinetics.
The interest of the model will also be investigated in cases involving convective or radiative boundary conditions, with possibly different values on the fibre and the matrix as the result of different emissivity for example.

References

[1] Y. Benveniste and T. Miloh, The effective conductivity of composites with imperfect thermal contact at constituent interfaces, Int. J. Eng. Sci. 24 (1986) 1537-1552.

[2] DPH. Hasselman and LF. Johnson, Effective Thermal Conductivity of Composites with Interfacial Thermal Barrier Resistance, J. Compos. Mater. 21 (1987) 508-515.

[3] S. Zhai, P. Zhang, Y. Xian, J. Zeng, B. Shi, Effective thermal conductivity of polymer composites: theoretical models and simulation models, Int. J. Heat Mass Transf. 117 (2018) 358–374.

[4] K. Dong, K. Liu, Q. Zhang, B. Gu, B. Sun, Experimental and numerical analyses on the thermal conductive behaviors of carbon fiber/epoxy plain woven composites, Int. J. Heat Mass Transf. 102 (2016) 501–517.

[5] M. Quintard and S. Whitaker, One- and two-temperature models for transient diffusion processes in two-phase systems, Adv. Heat Transf. 23 (1993) 369-464.

[6] A. Dobri, A. Tsiantis, T.D. Papathanasiou, Y. Wang, Investigation of transient heat transfer in multi-scale PCM composites using a semi-analytical model, Int. J. Heat Mass Transf. 175 (2021) 121389.

[7] G. Dusserre, A. Farrugia and T. Cutard, Enabling pseudo-ductility in geopolymer based glass-ceramics matrix composites by slurry dilution, Open Ceramics 7 (2021) 100156.

[8] D. Junger, M. Liebscher, J. Zhao, V. Mechtcherine, Joule heating as a smart approach in enhancing early strength development of mineral-impregnated carbon-fibre composites (MCF) made with geopolymer, Compos. Part A-Appl. Sc. 153 (2022) 106750.

[9] H.Y. Zhang, J.C. Liu, B. Wu, Mechanical properties and reaction mechanism of one-part geopolymer mortars, Constr. Build. Mater. 273 (2021) 121973.

[10] J. Cai, J. Pan, X. Li, J. Tan, J. Li, Electrical resistivity of fly ash and metakaolin based geopolymers, Constr. Build. Mater. 234 (2020) 117868.

[11] P. Payakaniti, S. Pinitsoonthorn, P. Thongbai, V. Amornkitbamrung, P. Chindaprasirt, Effects of carbon fiber on mechanical and electrical properties of fly ash geopolymer composite, Mater. Today: Proc. 5 (2018) 14017–14025.

[12] E. Chapelle, B. Garnier, B. Bourouga, Interfacial thermal resistance measurement between metallic wire and polymer in polymer matrix composites, InT. J. Therm. Sci. 48 (2009) 2221-2227.